



**Fermi National Accelerator Laboratory**

FERMILAB-PUB-92/356  
December, 1992

## Lattice QCD, the Quark Model, and Heavy-Light Wavefunctions

A. Duncan

Department of Physics and Astronomy  
University of Pittsburgh, Pittsburgh, PA 15620

E. Eichten

Fermi National Accelerator Laboratory  
P.O. Box 500, Batavia, IL 60510

H. Thacker

Department of Physics  
University of Virginia, Charlottesville, VA 22901

December 1, 1992

### **Abstract**

A multistate smearing method previously introduced allows a detailed study of the properties of heavy-light mesons in lattice QCD. The Coulomb gauge wave functions for the ground state, the first radially excited S-wave state, and the lowest P-wave states of a heavy-light meson are calculated in quenched approximation. The results are found to be in remarkably good agreement with the predictions of a simple relativistic quark model.

# 1 Introduction

The dynamics of QCD simplifies in two limits: (1) the usual chiral limit ( $m_q = 0$ ) and (2) the heavy quark limit ( $m_Q \rightarrow \infty$ )[1]. Heavy-light systems thus provide an ideal laboratory for lattice QCD studies. The development of lattice methods for studying heavy-light mesons has received much attention[2]. The static approximation ( $m_Q \rightarrow \infty$ ) in which the heavy quark propagator is replaced by a straight time-like Wilson line provides a framework which allows a quantitative study of masses, decay constants, mixing amplitudes, and electroweak form factors. Since heavy-light mesons have only one dynamical light (valence) quark, these systems are also well suited to the study of constituent quark ideas[3] and the chiral quark model[4].

The nonrelativistic (NR) potential model for heavy  $Q\bar{Q}$  mesons has been very successful in describing the properties of the  $c\bar{c}$  and  $b\bar{b}$  families of resonances.[5] Lattice calculations of the QCD potential[6] and direct simulation of heavy  $Q\bar{Q}$  systems on the lattice using either an improved Wilson action[7] or a NR fermion action[8] agree well with the phenomenological NR potential model. Therefore, one interesting dynamical question for heavy-light systems is the nature and extent of the deviation from the NR potential picture as the dynamical quark becomes light. In this note we report results of a numerical lattice study of this question. Our findings support a surprisingly simple answer. The Coulomb gauge wavefunctions[9] obtained in lattice QCD agree, within the accuracy of our calculations, with the results of a simple relativistic generalization of the NR quarkonium potential model. It is only necessary to replace the NR kinetic energy term in the Hamiltonian by its relativistic form, leaving the NR potential unchanged. The only adjustable parameter is a quark mass parameter  $\mu$ . This description holds down to fairly small values of the current quark mass, corresponding to a pion mass of approximately  $300 \text{ MeV}/c^2$ , well into the region where the NR description fails. In addition to their theoretical interest, our results have practical implications for future lattice studies. Precise lattice QCD calculations require the construction of operators which have large overlap with the hadronic state of interest and small overlap with other low-lying states. Our approach provides an optimal set of valence quark operators for heavy-light mesons.

In the next section we review the multistate smearing method[10] which was used to extract lattice wavefunctions, and we discuss the essential details of our lattice calculations. In section 3 we describe a lattice version of the relativistic quark model. In section 4 the wavefunctions for the relativistic

quark model are compared with those extracted from lattice QCD. Some implications of our results are discussed in section 5.

## 2 Wavefunctions in Lattice QCD

In actual lattice calculations, many practical issues must be addressed. In this section we focus on the issues of operator smearing. The properties of hadronic states are studied using correlation functions of operators which couple to the state. Originally local operators were used. More recently smeared (non-local) operators have been found to improve the ability to extract the masses of meson and baryon ground states[11]. Many of the recent studies have been done with configurations and propagators fixed in Coulomb gauge and operators which smear the position of the quark field uniformly over a spatial cube of variable size[12]. However a constant cube of any size is a very crude approximation to the ground state wavefunction[13]. Hence, the propagator generally has significant contamination from higher states out to times large compared to the inverse of the energy splitting between the ground state and the lowest excited state. This is a particular problem in the study of heavy-light correlators because they become noisy rather rapidly in time. Unfortunately, this is an unavoidable feature of heavy-light systems[14]. Recently a multistate smearing technique has been proposed[10] which allows the extraction of the properties of heavy-light states from relatively short times[15].

The basics of the multistate smearing method are simple. For example, consider the pseudoscalar channel. Let  $\Psi_{\text{smear}}^{(a)}(\vec{r})$  ( $a = 1, 2, \dots, N$ ) be a set of linearly independent, orthogonal wavefunctions with S-wave symmetry. These wavefunctions are generated by a Hamiltonian,  $H$  and ordered by eigenvalue,  $E^{(a)}$ . The basic multismear correlator,  $S^{(a)}$  ( $a = 1, 2, \dots, N$ ), is given by:

$$S^{(a)}(\vec{r}, T) = \sum_{\vec{r}'} \Psi_{\text{smear}}^{(a)}(\vec{r}', T) \langle q(\vec{r} + \vec{r}', T) Q^\dagger(\vec{r}', T) Q(\vec{r}', 0) q^\dagger(\vec{0}, 0) \rangle \quad (1)$$

The heavy quark operator,  $Q$ , simply generates a product of gauge links along the time direction.  $S^{(a)}$  is a  $3 \times 3$  matrix in color indices and a  $4 \times 4$  matrix in Dirac indices, the same as the light quark propagator.

For given quantum numbers and a well-chosen set of smearing wavefunctions it is possible to accurately extract the low-lying heavy-light states with

only a small number of smearing functions.

The investigation presented here used an existing set of 50 configurations (separated by 2000 sweeps) generated by ACPMAPS on a  $16^3 \times 32$  lattice at  $\beta = 5.9$ . The configurations were fixed to Coulomb gauge and light quark propagators with  $\kappa = .158$  were used. Only the four lowest energy smearing functions are included ( $N = 4$ ).

The appropriate smearing functions can be obtained by an iterative process:

- Start with a reasonable smearing function for the ground state. For our initial choice, an exponential  $\exp(-R/R_0)$  with  $R_0 = .5a$  was used.
- Measure the ground state wavefunction at moderate time  $T$ . The singlet piece of the wavefunction (obtained by projecting on the spin and color singlet piece of the smeared correlator  $S^{(1)}(\vec{r}, T)$ ) was measured at times  $(3 - 6)a$ .
- Tune the parameters in the Hamiltonian,  $H$  to give the best fit for the lowest eigenfunction to the measured ground state wavefunction.
- Generate the required number ( $N$ ) of smearing wavefunctions from this tuned  $H$ .
- Use this set of smearing functions to calculate the multismearred correlators.
- To take maximum advantage of these measurements, define a  $N \times N$  ( $4 \times 4$ ) coupling matrix,

$$C^{ab}(T) = \sum_{\vec{r}} \Psi_{\text{smear}}^{\dagger(b)}(\vec{r}) S^{(a)}(\vec{r}, T) \quad (2)$$

Diagonalizing the coupling matrix at each time  $T$  gives eigenvalues,  $\lambda^i(T)$ , which are related to the mass of the  $i^{\text{th}}$  heavy-light state by

$$\mathcal{E}^i(T) = -\log(\lambda^i(T))/\log(\lambda^i(T+1)) \quad (3)$$

and eigenvectors which give the coupling of the set of smearing functions to that  $i^{\text{th}}$  state.

- Finally, the improved wavefunctions for the heavy-light states can be used to retune the parameters in  $H$  and then the whole process repeated with better smearing functions.

A critical element in this procedure is the choice of the trial Hamiltonian  $H$  with appropriate parameters. In the next section we discuss our choice.

### 3 Relativistic Quark Model

The optimized wavefunctions obtained from our lattice data by the multistate smearing method turn out to be, within errors, the same as the eigenfunctions of a lattice version of the spinless, relativistic quark model Hamiltonian, which we will now define. In the absence of gauge fields, the free quark Hamiltonian can be exactly diagonalized by introducing momentum space creation and annihilation operators for quarks and antiquarks. In the continuum,

$$H_0 = \int \frac{d^3p}{(2\pi)^3} \sqrt{\vec{p}^2 + \mu^2} \sum_i \left[ \alpha_i^\dagger(p) \alpha_i(p) + \beta_i^\dagger(p) \beta_i(p) \right] \quad (4)$$

where the sum is over spin and color labels. In terms of the covariant quark propagator, the particle and antiparticle operators are associated with propagation forward and backward in time, respectively. Since  $H_0$  contains no pair creation ( $\alpha^\dagger \beta^\dagger$ ) terms, it is possible to formulate the eigenvalue problem as that of a one-body operator,

$$H_0 \rightarrow \sqrt{\mu^2 - \nabla^2} \quad (5)$$

If we now turn on the gauge interaction and introduce a heavy-quark, static color source, the description of the bound light quark becomes, in principle, drastically more complicated. We know that, in the limit  $\mu \gg \Lambda_{QCD}$  where the dynamical quark becomes heavy, the primary effect of the color source is to introduce a static, confining potential  $V(r)$  whose form is well-measured and consistently given by both  $Q\bar{Q}$  phenomenology and lattice QCD,

$$H_0 \rightarrow H = H_0 + V(r) \quad (6)$$

At this stage, the Hamiltonian can still be regarded as a one-body operator.[16] As the mass of the quark becomes light, one expects more complicated effects arising from the gauge interaction which render the Hamiltonian eigenvalue problem intractable. These effects include the creation of gluons and light  $q\bar{q}$  pairs, as well as the exchange of transverse and non-instantaneous gluons with the static source. (Note that  $q\bar{q}$  pairs arise even in quenched approximation, due to backward-in-time propagation of a valence quark.) From the numerical results presented in the next section, we conclude that these effects are relatively small, and that the heavy-light meson system is well-described by the Hamiltonian (6), which we will refer to as the spinless relativistic quark model (SRQM).

The construction of explicit eigenfunctions of the SRQM Hamiltonian is easily accomplished by a numerical procedure. First the operator  $H$  is discretized on a 3D lattice by replacing the spatial derivatives with finite differences. Thus the free lattice Hamiltonian has the form,

$$H_0 = \sqrt{\sum_i \hat{p}_i^2 + \mu^2} \quad (7)$$

where  $\hat{p}_i = \sin(p_i a)/a$ . The potential energy  $V(r)$  is just the static energy measured on the same configurations used to study the heavy-light spectrum. Then the resolvent operator  $(E - H)^{-1}$  acting on a source vector  $\chi$  is computed by a numerical matrix inversion (conjugate gradient) algorithm. Here  $\chi$  can be any vector that has nonzero overlap with the eigenstate of interest. Finally, the parameter  $E$  is varied to find the poles in the output vector  $(E - H)^{-1}\chi$ . The location of the pole is an eigenvalue of  $H$ , and its residue is the corresponding eigenfunction. In the next section we compare the wavefunctions obtained in this way from the SRQM Hamiltonian with the lattice QCD results.

## 4 Comparison of Wavefunctions

Using the four state smeared correlator described in section 2 an initial study for the S-wave channel was carried out. In the first pass (using an exponential smearing function for the ground state) the value  $\mu = .45$  was used. After some iterative improvement of the smearing functions, it was found that the value  $\mu = .20$  for the dimensionless mass parameter in the SRQM Hamiltonian gave the best agreement with the lattice QCD wavefunctions at  $\beta = 5.9, \kappa = .158$ . In Fig. 1 the LQCD wavefunction is plotted with the SRQM wavefunction. For comparison, the nonrelativistic (NR) Schrodinger wavefunction (obtained by replacing the relativistic kinetic term by  $p^2/2m$ ) is also plotted. The mass parameter in the NR Hamiltonian was adjusted to give the same slope at the origin in the ground state wavefunction. The effects of relativistic quark propagation are clearly seen in our data, since the corresponding nonrelativistic Schrodinger equation with a kinetic term  $p^2/2m$  fails to give an adequate description of the measured wave functions.

Notice that, for large  $r$ , the QCD and SRQM wavefunctions both fall exponentially. On the other hand, the NR wavefunction falls faster than exponentially ( $\exp(-\alpha r^{\frac{3}{2}})$ ), as expected from the behavior of the analytic solution in a pure linear potential (Airy function). This is a clear indication

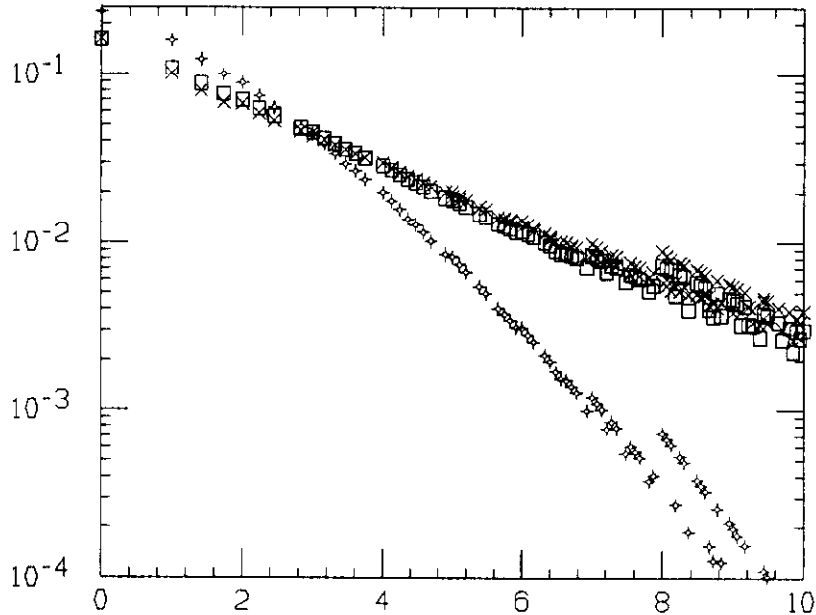


Figure 1: Comparison of the 1S state in LQCD ( $\times$ 's) with the NRQM ( $+$ 's) and the SRQM (boxes).

of relativistic effects, as faster than exponential fall of the wavefunction is inconsistent with the asymptotic behavior ( $\sim e^{-mr}$ ) of the nonlocal relativistic kinetic kernel (Fourier transform of  $\sqrt{p^2 + m^2}$ ).

Remarkably, by including the relativistic kinetic term, the SRQM wavefunctions are brought into excellent agreement with those of lattice QCD, without changing the potential from its nonrelativistic form.

In Fig. 2 we plot the excited 2S state from LQCD along with the corresponding wavefunctions from the SRQM and the NR model. The QCD wavefunction is somewhat more peaked at the origin, however, the overall agreement between QCD and the SRQM is excellent. Here, there are no adjustable parameters,  $\mu$  being already fixed from the 1S state fit.

Finally, in Fig. 3 we show some preliminary results of a study of the 1P state. The data points depict the evolution of the P-wave LQCD radial wavefunction extracted from time slices  $T = 2$ ,  $T = 4$ , and  $T = 6$ , starting with an approximate guess for the initial smearing function. The ansatz

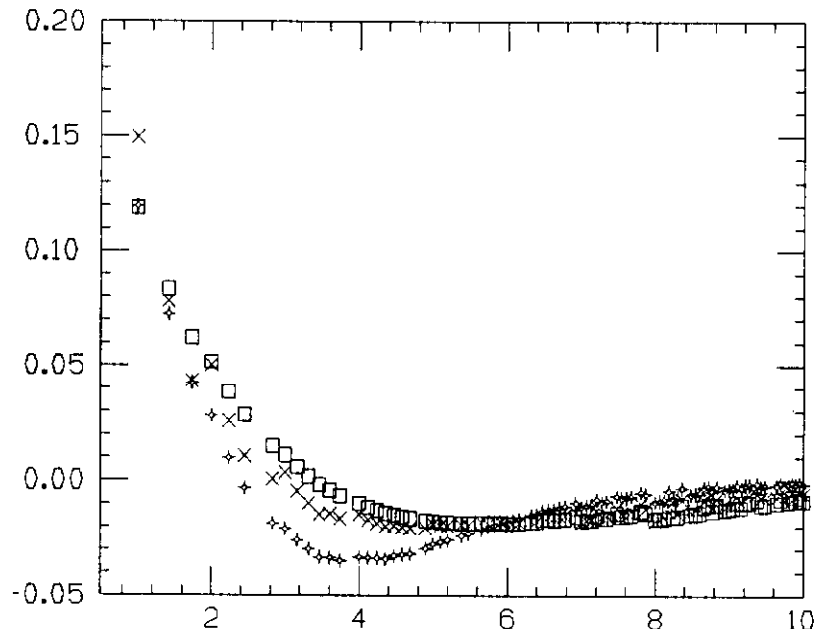


Figure 2: Comparison of the 2S state in LQCD ( $\times$ 's) with the NRQM ( $+$ 's) and the SRQM (boxes).

for the initial smearing function used here was a simple  $re^{-\alpha r}$  form. As the LQCD wavefunction evolves in Euclidean time, it appears to approach a true eigenstate whose wavefunction again agrees well with the SRQM result, with no adjustable parameters.

## 5 Discussion

In the heavy-light system, we have been able to calculate accurate lattice QCD wavefunctions by the multistate smearing method. These wavefunctions are in remarkable agreement with the wavefunctions generated by a spinless relativistic quark model (SRQM) with a potential (static energy) calculated from the same lattice configurations. By adjusting a single reduced mass parameter in the SRQM, we obtain good agreement with the measured lattice QCD wavefunctions for not only the ground state, but also for the lowest lying P-wave states and the first radially excited S-wave. Ad-

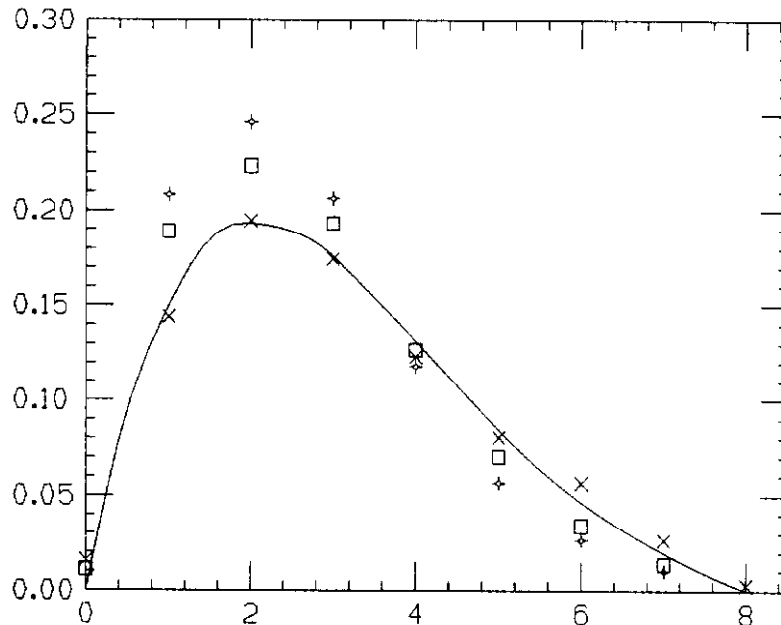


Figure 3: The 1P state in LQCD extracted from  $T=2$  (+'s),  $T=4$  (boxes), and  $T=6$  (x's). For comparison the SRQM wavefunction (solid line) is also shown.

ditional studies are in progress using a variety of lattice sizes, gauge coupling strengths, and light quark masses. Preliminary results of these studies are fully consistent with the conclusions presented here.

The agreement with the SRQM suggests that the relativistic propagation of the light valence quark is the most important effect which must be included in a description of heavy-light mesons. Other field theoretic effects such as the presence of multibody components of the wavefunction (containing gluons along with light  $q\bar{q}$  pairs) are of less quantitative importance in determining the shape of the valence quark wavefunction. Further numerical studies of the connection between QCD and the relativistic quark model are planned.

## 6 Acknowledgements

We thank George Hockney, Aida El-Khadra, Andreas Kronfeld, and Paul Mackenzie for joint lattice efforts without which this analysis would not have been possible. We also thank Chris Quigg for useful discussions. The numerical calculations were performed on the Fermilab ACPMAPS computer system developed by the CR&D department in collaboration with the theory group. This work was supported in part by the U.S. Department of Energy under grant No. DE-AS05-89ER40518 and National Science Foundation under grant No. PHY-90-24764.

## References

- [1] See for example: H. Georgi, in *Perspectives in the Standard Model*, Proceedings of the 1991 Theoretical Advanced Study Institute in Elementary Particle Physics, eds. R. K. Ellis, C. T. Hill, and J. D. Lykken (World Scientific, Singapore, 1992) p. 589.
- [2] For a review of lattice heavy-light systems see: E. Eichten, in *Lattice 90*, Nucl. Phys. B(Proc.Suppl.) **20** (1991) 475.
- [3] J. D. Bjorken, SLAC preprint SLAC-PUB-5278 (1990).
- [4] A. Manohar and H. Georgi, Nucl. Phys. B**234** (1984) 189.
- [5] For a review see W. Kwong, J. L. Rosner, and C. Quigg, Ann. Rev. Nucl. Part. Sci. **37** (1987), 35.
- [6] G. S. Bali and K. Schilling, Wuppertal Preprint WUB 92-29 (1992).
- [7] P. Mackenzie, in *Lattice 91*, Nucl. Phys. B(Proc.Suppl.) **26** (1992) 369; A. El-Khadra, *ibid.* 372.
- [8] B. Thacker and G. P. Lepage, Phys. Rev. D**43** (1991) 196; G. P. Lepage et. al, Cornell Preprint CLNS-92-1136 (1992).
- [9] Light hadron wavefunctions were first studied by S. Gottlieb, in *Advances in Lattice Gauge Theory*, (World Scientific, Singapore, 1985) p.92; D. Weingarten and B. Velikson, Nucl. Phys. B**249** (1985) 433; For recent studies, see W. Hecht et. al., Univ. of Colorado preprint COLO-HEP-291 (1992) and references contained therein.

- [10] A. Duncan, E. Eichten, and H. Thacker, in *Lattice 91* Nucl. Phys. **B**(Proc. Suppl) 26 (1992) 394.
- [11] P. Bacilieri et. al., Nucl. Phys. **B317** (1989) 509.
- [12] See for example: C. Allton et. al., Nucl. Phys. **B376** (1992) 172.
- [13] S. Hashimoto and Y. Saeki, Mod. Phys. Lett. **A7** (1992) 387.
- [14] C. Bernard, C. Heard, J. Labrenz, and A. Soni, in *Lattice 91* Nucl. Phys. **B**(Proc. Suppl) 26 (1992) 384; also see ref.[10].
- [15] For applications of this smearing technique to nonrelativistic systems see: A. Duncan, E. Eichten, G. Hockney, and H. Thacker, *Lattice 91* Nucl. Phys. **B**(Proc. Suppl) 26 (1992) 398.
- [16] E. E. Salpeter, Phys. Rev. **87**, (1952) 328.